MEAN TOPOLOGICAL EVOLUTION IN COMPRESSIBLE TURBULENT BOUNDARY LAYER

You-Biao Chu & Xi-Yun Lu[a)]

Department of Modern Mechanics, University of Science and Technology of China, Hefei, Anhui 230026, China

Summary The mean topological evolution of fluid particles in a compressible turbulence boundary layer is analyzed by means of conditional mean trajectories (CMTs) for the evolution of the invariants of the velocity gradient tensor (VGT), calculated by the mean rate of change of the invariants in the (R_A, Q_A, P_A) invariants space. The results of the CMTs in the invariants space show that the trajectories orbit around the origin and spiral inward in the log layer, while exhibit a limit cycle behavior in the buffer layer.

CONDITIONAL MEAN TRAJECTORY

Following the topological approach introduced by Chong, Perry & Cantwell (1990) the invariants of the VGT can be used to classify the local topology of any point in the flow [1], within a basis of critical point theory. In this paper, the Lagrangian evolution of the invariants of the VGT is studied using CMTs. These CMTs are derived using the concept of the conditional mean time rate of change of invariants [2, 3] calculated from a direct numerical simulation (DNS) of compressible turbulent boundary layer ($Ma = 2$, $Re_\theta = 1650 \sim 1875$) performed by Wang & Lu (2011) [4].

The VGT $A_{ij} = \partial u_i/\partial x_j$ has the characteristic equation: $\lambda_i^3 + P_A\lambda_i^2 + Q_A\lambda_i + R_A = 0$, where λ_i are the eigenvalues of **A** and, P_A, Q_A and R_A are the first, second and third tensor invariants respectively. **S** is the symmetric strain-rate tensor, **W** is the skew-symmetric rotation-rate tensor, Q_W is the second tensor invariant of **W** and positive definite, Q_S is the second tensor invariant of **S** and negative definite.

Figures 1(a) and 1(b) show CMTs and iso-surfaces of the joint probability density functions ($jPDF$) of the invariants of the VGT in the (R_A, Q_A, P_A) space for the buffer and log layer, respectively. The values of R_A, Q_A and P_A along the trajectory are plotted versus integration time in figures 1(c) and 1(d) for the log and buffer layer. In the log layer, the trajectory orbits around the origin and spiral inward. This result agrees with the finding of Elsinga & Marusic (2010) [3] for an incompressible boundary layer. It is interesting to note that a limit cycle behavior is exhibited in the buffer layer. As shown in figures 1(b) and 1(d), the trajectory colored in blue demonstrates that data outside the limit cycle spirals inward along the trajectory, while the trajectory colored in black represents that data inside the limit cycle spirals outward along the trajectory. On average, the local topology of fluid particles near the limit cycle will change from Unstable Node/Saddle/Saddle (UN/S/S) to Stable Node/Saddle/Saddle (SN/S/S), to Stable Focus/Stretching (SF/S), to Stable Focus/Compressing (SF/C), and to Unstable Focus/Compressing (UF/C).

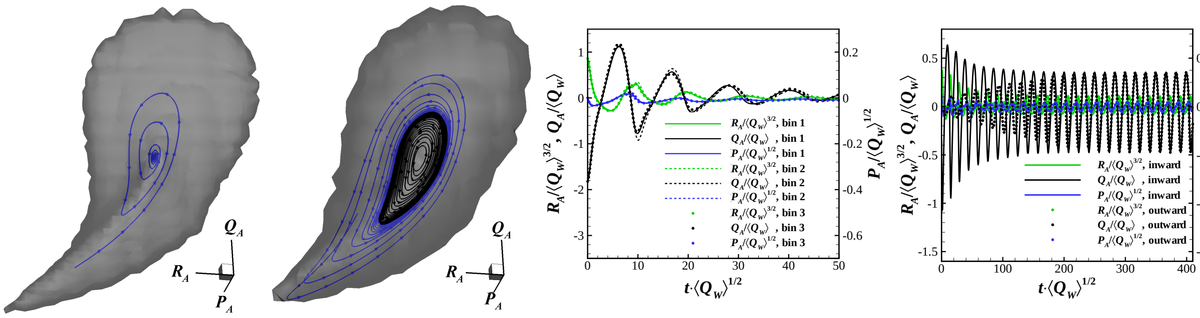

Figure 1. CMTs and iso-surfaces of $jPDF$ of the invariants and time evolution of R_A, Q_A and P_A along CMTs. (*a*) and (*c*) for the log layer, (*b*) and (*d*) for the buffer layer. $jPDF = 0.001$. Bin 1: $0.01 \times 0.1 \times 0.004$; bin 2: $0.02 \times 0.05 \times 0.004$; bin 3: $0.02 \times 0.1 \times 0.002$.

DYNAMICS ANALYSIS OF MEAN TOPOLOGICAL EVOLUTION

The time evolution of **A** following fluid particles can be obtained by taking the gradient of the Navier-Stokes equations (see, e.g. [5, 6]). The resulting equation reads

$$\frac{DA_{ij}}{Dt} + A_{ik}A_{kj} = -\frac{1}{\rho}H_{ij} - \frac{1}{\rho^2}B_{ij} + V_{ij} \tag{1}$$

where $\frac{D}{Dt}$ stands for the Lagrangian material derivative, B_{ij}, V_{ij} and H_{ij} represent the baroclinic tensor, viscous tensor and pressure Hessian tensor, respectively, and are defined as $H_{ij} = \frac{\partial^2 p}{\partial x_i \partial x_j}$, $B_{ij} = \frac{\partial p}{\partial x_i}\frac{\partial \rho}{\partial x_j}$, $V_{ij} = \frac{\partial}{\partial x_j}\left(\frac{1}{\rho}\left(\frac{\partial \sigma_{ik}}{\partial x_k}\right)\right)$, and σ_{ik} is the viscous stress tensor. Equation 1 then yields the evolution equations for P_A and Q_A,

$$\frac{DP_A}{Dt} = \frac{1}{2}P_A^2 - 2Q_A + \frac{1}{\rho}\mathrm{tr}(\mathbf{H}) + \frac{1}{\rho^2}\mathrm{tr}(\mathbf{B}) - \mathrm{tr}(\mathbf{V}) = OP + OQ + OH + OB + OV, \tag{2}$$

[a)] Corresponding author. E-mail: xlu@ustc.edu.cn.

$$
\begin{aligned}
\frac{DQ_A}{Dt} &= 3\mathbf{S}:\mathbf{W}^2+\mathbf{S}:\mathbf{S}^2+P_A\left(\frac{1}{2}P_A^2-2Q_A\right)-\left[P_A\mathrm{tr}(\mathbf{V})+\mathbf{S}:\left(\frac{\mathbf{V}+\mathbf{V}^T}{2}\right)+\mathbf{W}:\left(\frac{\mathbf{V}^T-\mathbf{V}}{2}\right)\right] \\
&\quad +\frac{1}{\rho^2}\left[P_A\mathrm{tr}(\mathbf{B})+\mathbf{S}:\left(\frac{\mathbf{B}+\mathbf{B}^T}{2}\right)+\mathbf{W}:\left(\frac{\mathbf{B}^T-\mathbf{B}}{2}\right)\right]+\frac{1}{\rho}\left(P_A\mathrm{tr}(\mathbf{H})+\mathbf{S}:\mathbf{H}\right) \\
&= VS+SI+DP+VA+BE+PH. \qquad (3)
\end{aligned}
$$

The mean Q_A budget terms along P_A are reported in figure 2(*c*). It is indicated that the vortex stretching term (VS) is balanced primarily by the self-interaction of the strain-rate tensor (SI) in the buffer layer due to the competition between enstrophy and dissipation with $Q_A = Q_W + Q_S$ [4]. The contribution of the pressure Hessian tensor (PH) to Lagrangian evolution of Q_A is the largest one as compared to the other budget terms, especially in a weaker compression region. The sum of all the budget terms, marked by red solid line in figure 2(c), shows that the second invariant of fluid particle tends to increase in the expansion region and decrease in the compression region, as shown in figure 2(*a*,*b*). The local topology of fluid particles in (R_A,Q_A) plane is considered by means of neglecting the slight change of dilatation. On average, the local topology of fluid particles in the expansion region changes from UN/S/S to SF/S and Unstable Focus/Stretching(UF/S) through SN/S/S and UF/C, respectively, while the local topology of fluid particles in the compression region changes from SF/S to SF/C to UF/C to UN/S/S or from SF/S to SN/S/S to UN/S/S. Correspondingly, the local topology of fluid particles near the limit cycle in the buffer layer will changes from UN/S/S to SN/S/S to SF/S in the expansion region, while from SF/S to SF/C to UF/C to UN/S/S in the compression region.

Figure 3(a) shows conditional mean time rate of change vectors of Q_A and R_A in the 'incompressible' region with P_A around zero in the buffer layer. The local topology of fluid particles changes around the origin in clockwise direction, which is consistent with the result of incompressible case [2-3, 7]. The mean P_A budget terms along P_A are given in figure 3(*b*-*c*). It is found that the contribution of Q_A (OQ) is balanced primarily by the effect of the pressure Hessian tensor (OH), with $OQ + OH = 0$ for incompressible case. As shown in figure 3, on average the particles in the 'incompressible' and enstrophy dominated region tend to be compressed and those in the 'incompressible' and dissipation dominated region tend to be expanding. It is also identified that the results exhibited in this section are similar to those of the log layer.

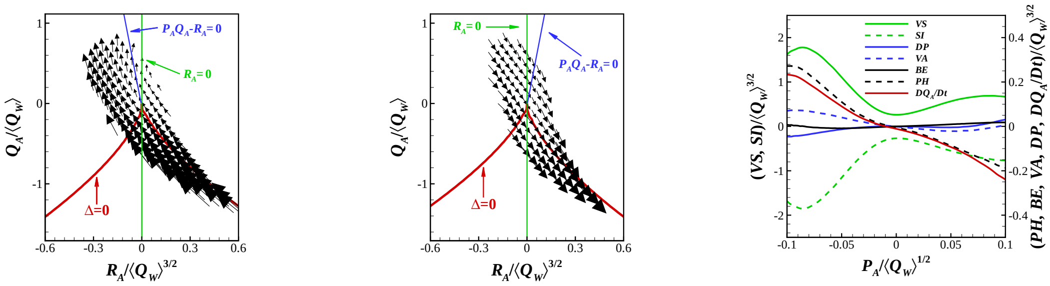

Figure 2. Conditional mean time rate of change vectors of Q_A and R_A in the buffer layer for (*a*) $P_A = -0.1$ and (*b*) $P_A = 0.1$. (*c*) Distributions of the mean Q_A budget terms versus P_A.

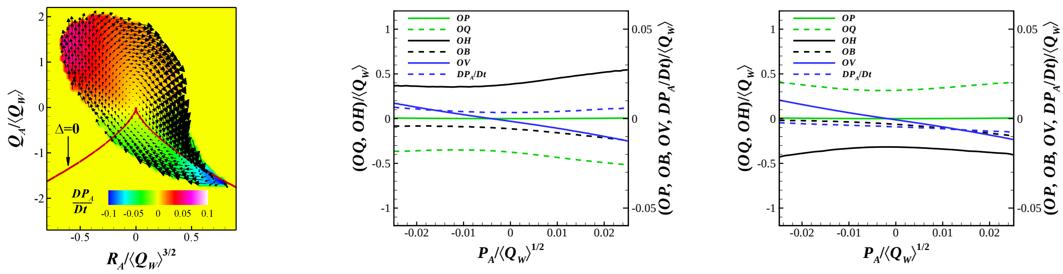

Figure 3. (*a*) Conditional mean time rate of change vectors of Q_A and R_A in the buffer layer for $P_A = 0.0$. Distributions of the mean P_A budget terms versus P_A for: (*b*) $Q_A > 0$ and (*c*) $Q_A < 0$.

References

[1] Chong M. S., Perry A. E., Cantwell B. J.: A General Classification of Three-dimensional Flow Fields. *Phys. Fluids A* **2(5)**:756–777, 1990.

[2] Ooi A., Martin J., Soria J., Chong M. S.:A Study of the Evolution and Characteristics of the Invariants of the Velocity-gradient Tensor in Isotropic Turbulence. *J. Fluid Mech.* **381**:141–174, 1999.

[3] Elsinga G. E., Marusic I.:Evolution and Lifetimes of Flow Topology in a Turbulent Boundary Layer. *Phys. Fluids* **22**:015102, 2010.

[4] Wang L., Lu X.-Y.: Flow Topology in Compressible Turbulent Boundary Layer. *J. Fluid Mech.* (**submitted**).

[5] Pirozzoli S., Grasso F.:Direct Numerical Simulations of Isotropic Compressible Turbulence: Influence of Compressibility on Dynamics and Structures. *Phys. Fluid* **16**:4386–4407, 2004.

[6] Meneveau C.: Lagrangian Dynamics and Models of the Velocity Gradient Tensor in Turbulent Flows. *Annu. Rev. Fluid Mech.* **43**:219–245, 2011.

[7] Bermejo-Moreno I., Atkinson C., Chumakov S., Soria J., Wu X.:Flow Topology and Non-local Geometry of Structures in a Flat-plate Turbulent Boundary Layer. *Proceedings of the Summer Program 2010*.